GENERAL RESEARCH

Transport Properties of Perfluoroalkanes Using Molecular Dynamics Simulation: Comparison of United- and Explicit-Atom Models

Clare McCabe,*,[†] **Dmitry Bedrov,[‡] Oleg Borodin,[‡] Grant D. Smith,[‡] and Peter T. Cummings[§,||]**

Department of Chemical Engineering, Colorado School of Mines, Golden, Colorado 80401, Department of Materials Science & Engineering and Department of Chemical & Fuel Engineering, University of Utah, Salt Lake City, Utah 84112, Department of Chemical Engineering, Vanderbilt University, Nashville, Tennessee 37235, and Chemical Technology Division and Nanomaterials Theory Institute, Oak Ridge National Laboratory, Oak Ridge, Tennessee 37831-6110

We compare the results of an explicit-atom model (Borodin, O.; Smith, G. D.; Bedrov, D. *J. Phys. Chem. B* **2002**, *106*, 9912–9922) for perfluoralkanes with those of a united-atom model (Cui, S. T.; Siepmann, J. I.; Cochran, H. D.; Cummings, P. T. *Fluid Phase Equilib.* **1998**, *146*, 51–61) in the prediction of transport properties for short perfluoralkanes. The predicted viscosities from the two force fields are compared against each other and with experiment or correlations of experimental data. We find that the explicit-atom model predicts the Newtonian viscosity of short perfluoroalkane molecules in excellent agreement with experimental data and, in most cases, within experimental error, whereas the united-atom model underpredicts the Newtonian viscosity. Additional dynamical properties, including the diffusion coefficients from both models, are also reported.

1. Introduction

Flurorocarbons are important to a wide range of industrial (for example, as refrigerants, as solvents[1] and surfactants,[2–5] and as high-performance lubricants[6]) and medical (for example, as artificial blood or synthetic oxygen carriers and as fluids in eye surgery and in the treatment of burns[7,8]) applications and, consequently, are of interest in a number of research fields. Hence, the development of accurate and reliable models for fluorocarbons that would enable reliable, quantitative predictions of different thermophysical properties is of fundamental interest to a broad community.

It is widely recognized that the primary limitation to the practical application of simulation methods to industrial processes is force-field development and validation.[9–11] Force fields for hydrocarbon molecules are very well established, with several potential models available in the literature (for example, see refs 12–21 and references therein) that are capable of accurately predicting structural, dynamic, and thermodynamic (including phase equilibrium behavior) properties. In the parametrization process, ab initio quantum chemistry calculations are used to determine details of the intramolecular potential, whereas state properties, such as densities and vapor–liquid coexistence data, are generally used to fit the nonbonded dispersion interactions, usually to a Lennard-Jones or exponetial-6 functional form. Early hydrocarbon models used united-atom representations of the molecules (see, for example, refs 12, 13, and 16–19), in which each carbon atom and its hydrogens are treated as a single interaction site, whereas more recent work has focused on explicit-atom descriptions,[14,15,20] in which each atom in the molecule is explicitly described. However, although progress has been made in the development of transferable potential models for thermodynamic property estimation, similar developments for quantitative transport property prediction has lagged behind. In previous work in a series of publications, Cummings and co-workers[22–33] demonstrated both the inadequacies and successes of united-atom (UA) force fields parametrized for phase equilibria calculations when applied to the prediction of viscosity.[31,32,34] To summarize these results, UA force fields have been shown to underpredict the viscosity but to capture quite well the temperature dependence (measured by the kinetic viscosity index)[25,30,31] and pressure dependence (measured by the pressure–viscosity coefficient).[32]

In a limited study of both linear (C4–C12) and branched (C3–C5 backbones) alkanes, Allen and Rowley[35] compared the viscosities predicted using the OPLS (optimized potential for liquid simulations) UA and explicit-atom (EA) models. The torsional motion was the only intramolecular interaction included because, in both models, the bond lengths and bond angles were

---

* To whom correspondence should be addressed. E-mail: cmccabe@mines.edu.
† Colorado School of Mines.
‡ University of Utah.
§ Vanderbilt University.
|| Oak Ridge National Laboratory.

fixed to reduce the simulation time. This approximation alone is seen to have a significant impact on the predicted viscosities. With this assumption, they found that the UA model underpredicted the viscosity and the EA model overestimated the viscosity. The underestimation and overestimation were comparable in magnitude. By optimizing the diameter of the hydrogen atom in the model, they were able to obtain predicted viscosities within 10–20% of the experimental value. Hence, although this is a comparison between UA and EA models, the definitiveness of the comparison is obscured by the assumption of rigid bond lengths and rigid angles. We are unaware of any broad comparison of viscosity prediction using explicit-atom models for hydrocarbons with experiment or with their united-atom counterparts.

In comparison to hydrocarbons, simulation studies and force-field development for fluorinated molecules, such as the perfluoroalkanes, is much less advanced, for both thermodynamic and transport property estimations. Hence, the range of potential models available in the open literature that have been purposely designed to model perfluoroalkanes is limited.[15,36–50] Two of these models deserve particular attention. The groups of Cummings and Siepmann postulated two independently developed united-atom models for perfluoroalkanes optimized for fluid phase equilibrium calculations of the pure liquids.[48] For both models, good agreement was obtained with experimental data for the critical temperatures and densities and the saturated liquid densities of perfluoropentane, perfluorooctane, and perfluorodecane.[48] Note that neither of these force fields contains partial charges. Although longer-chain molecules were studied, further testing of the potential model against experimental data on pure perfluoroalkanes was not possible, as no experimental data were available beyond $C_{10}F_{22}$. However, the models were found to accurately predict phase equilibria in perflouroalkane/carbon dioxide mixtures[51] and provided the basis for the force fields used in a successful series of simulations of reverse micelles in supercritical carbon dioxide.[52,53] Borodin et al.[50] recently proposed an ab initio based explicit-atom force field for simulations of perfluroalkanes obtained by fitting the conformational energetics and geometries of perflouorobutane and perfluoropentane.[50] The transferability of the model was then demonstrated by comparing the conformational energetics of perfluorohexane predicted using the force field with that obtained from ab initio calculations. In contrast to the explicit-atom potential model for perfluroalkanes proposed by Jorgensen,[49] the Borodin force field does not contain partial charges. This is a significant advantage given the substantial reduction in computational time over systems with long-range Coulombic interactions. We note that neither the united-atom potentials of the Cummings and Siepmann groups[48] nor the explicit-atom model of Borodin et al.[50] was designed to accurately predict transport properties in general, and viscosity in particular. Nevertheless, many of the applications of fluorocarbons noted at the beginning of this article involve transport properties (viscosity and diffusivity).

Hence, in this work, we compare the transport property predictions of the explicit-atom model[50] with those of the united-atom potential model (model T from ref 48). We denote these models EA and UA, respectively. Although one of our previous studies[34] suggested

Table 1. Details of the State Points Studied

| molecule | temperature (K) | density^a (g cm^{-3}) | |
		experiment/UA model	EA model
C_4F_{10}	200	1.817	1.786
	260	1.636	1.643
	298	1.499	1.507
C_5F_{12}	215	1.855	1.813
	298	1.604	1.591
C_6F_{14}	298	1.674	1.663
	323	1.606	1.590
C_7F_{16}	298	1.706	1.710
	318	1.652	1.655

^{a} Densities correspond to 0.1 MPa pressure. For the UA model, experimental densities were used; for the EA model, the densities are calculated.

that a UA model might be inadequate for predicting the viscosities of perfluoroalkanes, this preliminary conclusion needs to be explored, given that, wherever possible, a UA model is to be preferred over a EA one because of the significantly lower computational cost. Additionally, judging from our previous simulation studies of the viscosity of hydrocarbon molecules with UA models (see, for example, refs 23, 25, 30, 32, 54, and 55), it is not unexpected that a UA model will underpredict the Newtonian viscosities of perfluoroalkanes compared to experiment; the interesting question is whether the state dependence of the predicted viscosity is captured well, thereby enabling the use of a UA description.

The rest of the paper is organized as follows: In section 2, we describe the potential models employed in this work, and in section 3 we provide details of the simulations performed. In section 4, we present the results and a comparison of the performance of the EA and UA models in the prediction of transport properties.

2. Simulation Details

The UA and EA force fields used in this study are described in detail elsewhere.[34,48,50] With the UA model, both equilibrium molecular dynamics (EMD) and nonequilibrium molecular dynamics (NEMD) simulations were performed in the *NVT* ensemble at densities obtained from experiment. The perfluoroalkanes were simulated under planar Couette flow using the SLLOD equations of motion with a Nosé thermostat.[56] A multiple-time-step technique[22,57] was used to integrate the equations of motion, with all of the intramolecular interactions being treated as fast motions and the intermolecular interactions as slow motions. For the fast-mode motions, a time step of 0.7 fs was used, and for the slow mode motions, the time step was 7 fs. A spherical potential cutoff of 2.5σ (11.5 Å) was used in all united-atom model simulations. The simulation cell contained 200 molecules in a cubic box, equilibrated initially using techniques described elsewhere.[32] The technical details of the EMD and NEMD simulations are identical, the only difference being the use of Lees–Edwards boundary conditions to describe the shear field in the NEMD simulations. The run times for the NEMD simulations varied from 5 to 30 ns depending on the magnitude of the strain rate being used. For the calculation of equilibrium properties with the EMD method, the production run was generally 10 ns.

For the EA model, isothermal–isobaric (*NpT*) equilibrium molecular dynamics simulations were performed for 2 ns to establish the equilibrium densities, which are reported in Table 1. The Nosé–Hoover[56]

thermostat and barostat were used to control the temperature and pressure. Dispersion interactions were truncated at 10 Å. An explicit reversible multiple-time-step integrator with time steps of 0.75 fs for bonding, bending, and torsional motion; 1.5 fs for nonbonded interactions within 6 Å; and 3.0 fs for nonbonded interactions between 6 and 10 Å was used.[58] For each molecule and each state condition, isothermal–isochoric (*NVT*) production runs of 8 ns duration were then performed using the Nosé–Hoover thermostat[56] with an integration step size of 1.0 fs at the densities obtained from the *NpT* simulations. Each system contained 200 molecules, except for systems of C_7F_{16}, which had 160 molecules in the simulation cell. The standard SHAKE algorithm[59] was used to constrain bond lengths.

During the NEMD simulations, the strain-rate-dependent viscosity was calculated using the usual Irving–Kirkwood expression for the pressure tensor.[60] The zero-shear or Newtonian viscosity can then be estimated from the NEMD simulation data by averaging the values of the viscosity at strain rates that appear to fall within the Newtonian plateau. In EMD simulations using the UA models, the viscosity η was calculated via the Green–Kubo formula involving the integral of the stress–stress autocorrelation functions determined during the simulation, viz[61]

$$\eta = \frac{V}{10 k_B T} \lim_{\tau \to \infty} \int_0^\tau dt \sum_{\alpha=x}^{z} \sum_{\beta=x}^{z} q_{\alpha\beta} \langle P_{\alpha\beta}(t) \, P_{\alpha\beta}(0) \rangle \quad (1)$$

where V is the volume of the system, k_B is the Boltzmann constant, T is the temperature, $q_{\alpha\beta} = 1 + \delta_{\alpha\beta}/3$, and t is time. The quantity $P_{\alpha\beta}(t)$ is the value of the $\alpha\beta$ off-diagonal component, with α, $\beta = x$, y, z, of the traceless symmetric stress tensor at time t, and so, $P_{\alpha\beta}(t) \, P_{\alpha\beta}(0)$ is the stress–stress autocorrelation function and $\langle P_{\alpha\beta}(t) P_{\alpha\beta}(0) \rangle$ is its ensemble average (indicated by $\langle ... \rangle$) measured during the course of the simulation. For the EA models, the Einstein (time-integrated) form of the Green–Kubo relation in the form proposed by Mondello and Grest[62] was used

$$\eta = \lim_{t \to \infty} \frac{V}{12 k_B T t} \left\langle \sum_{\alpha=x}^{z} \sum_{\beta=x}^{z} [\Delta A_{\alpha\beta}(t)]^2 \right\rangle \quad (2)$$

where

$$\Delta A_{\alpha\beta}(t) = \int_0^t P_{\alpha\beta}(t') \, dt' \quad (3)$$

It was shown by Mondello and Grest that eqs 2 and 3 give the same results as the Green–Kubo formulation for MD simulations of short-chain alkanes. For the EA model, we considered both formulations for the shear viscosity of perfluoroalkanes and found the results to differ by 2% or less.

In addition, the self-diffusion coefficient, *D*, was computed during EMD simulations using the standard Einstein relationship

$$D = \lim_{t \to \infty} \frac{\langle [\mathbf{R}_{cm}(t) - \mathbf{R}_{cm}(0)]^2 \rangle}{6t} \quad (4)$$

where $\mathbf{R}_{cm}(t) - \mathbf{R}_{cm}(0)$ is the time-dependent center-of-mass displacement of a given molecule.

3. Results and Discussion

Using both the UA and EA potential models, we have studied a number of short perfluoroalkane molecules,
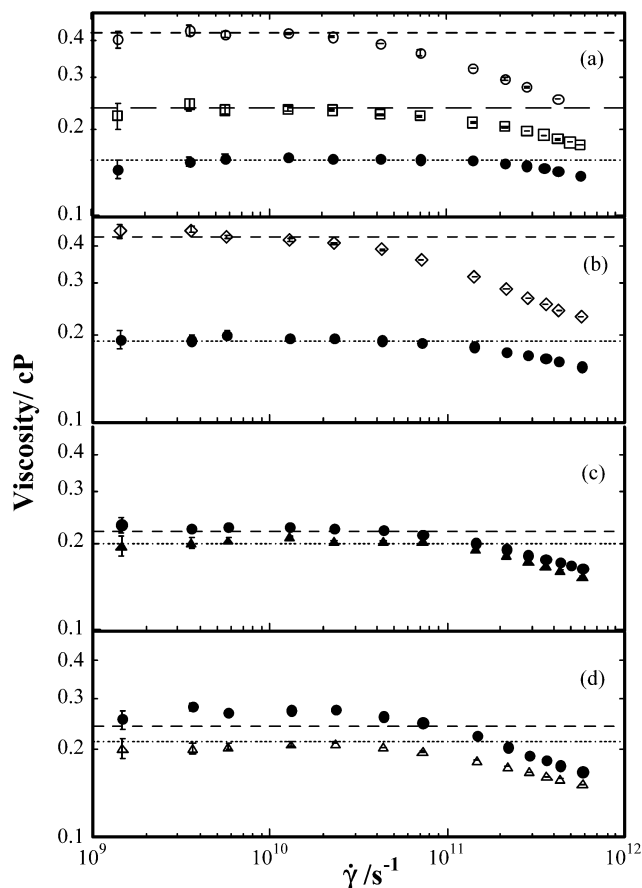

Figure 1. Strain-rate-dependent viscosity for (a) perfluorobutane, (b) perfluoropentane, (c) perfluorohexane, and (d) perfluoroheptane predicted using the UA model at state points given in Table 1. The horizontal lines correspond to the Newtonian viscosity calculated from EMD simulations. The temperatures are as follows: 200 K (○), 260 K (□), 298 K (●), 215K (◇), 323K (▲), 318 K (△).

namely, perfluorobutane, perfluoropentane, perfluorohexane, and perfluoroheptane, at the state points given in Table 1. For each state point, we determined the Newtonian viscosity and the self-diffusion coefficient. Because we performed both EMD and NEMD simulations with the united-atom model, the strain-rate-dependent viscosity was also determined.

The results from the UA and EA models are presented for the viscosity and comparisons between the results obtained and experimental data are discussed before the other calculated transport properties are reported. In Figure 1a, we present a log–log plot of the strain-rate-dependent viscosity of perfluorobutane over a temperature range of ~100 K at state points given in Table 1. In the figure, the horizontal lines correspond to the Newtonian viscosity obtained from the Green–Kubo formula, eq 1. We can see from the figure that the viscosity shows shear-thinning behavior at high strain rates and a Newtonian plateau at the lowest strain rates. The onset of shear thinning as the strain rate increases occurs at higher strain rates for the higher temperatures studied, consistent with earlier work. The zero-shear viscosity was estimated from the NEMD simulation data by averaging the values at strain rates within the Newtonian plateau. The numerical value from this procedure at each state point is given in Table 2, along with experimental values for comparison.[63,65] Several conclusions concerning the UA results are clear: First, there is very good agreement between the

Table 2. Predicted Values for the Newtonian Viscosity from Experiment and the EMD and NEMD Simulations

molecule	temp (K)	viscosity (cP)				
			UA		EA	EA/UA
		experiment	EMD	NEMD	EMD	EMD
C_4F_{10}	200	1.46	0.408	0.406	1.66	4.1
	260	0.52	0.223	0.224	0.63	2.8
	298	0.34	0.157	0.154	0.36	2.3
C_5F_{12}	215	1.98	0.428	0.425	2.02	4.7
	298	0.46	0.204	0.190	0.56	2.7
C_6F_{14}	298	0.66	0.220	0.224	0.70	3.2
	323	0.47	0.195	0.201	0.51	2.6
C_7F_{16}	298	0.89	0.234	0.264	1.10	4.7
	318	0.66	0.201	0.203	0.89	4.4

prediction of the Newtonian viscosity from the EMD and the NEMD simulation methods. Second, the UA model substantially underpredicts the zero-shear viscosity. Similar results and conclusions were found for perfluoropentane (Figure 1b), perfluorohexane (Figure 1c), and perfluoroheptane (Figure 1d) with the corresponding Newtonian viscosities given in Table 2.

As discussed in the Introduction, we had anticipated that the UA model would underpredict the viscosity; however, the underprediction appears to be to a larger degree than that obtained using a UA model for hydrocarbons. This result is perhaps not surprising if one compares the size of a H atom to that of a F atom. Whereas it might be reasonable to collapse a CH_3 or CH_2 group into a single, spherical, united-atom site, it is clearly a greater approximation for perfluoroalkane molecules. The results of the EMD simulations using the EA model for each molecule are also presented in Table 2, from which we note that the agreement with experimental data is very good and, in some cases, within experimental error.

In Figures 2 and 3, we compare the predicted temperature and chain-length dependences for both models with the experimental data. We see from Figure 2 that the EA model captures the change in viscosity with temperature well. For the UA model, the slope of the line characterizing the influence of temperature is in reasonable agreement with experiment. If one examines the change in viscosity as a function of chain length (Figure 3) for both models compared to experiment, the UA model significantly underpredicts the dependence of viscosity on chain length, in contrast to the case for alkanes, for which the chain-length dependence is predicted quite well by UA models. Unfortunately, we do not have any experimental data for the viscosity as a function of pressure for perfluoroalkanes and so are unable to comment on the pressure dependence; however, previous studies for hydrocarbons using UA models showed accurate behavior with changes in both temperature and pressure,[25,31,32] suggesting that the UA model in this work will do a reasonable job of capturing the influence of changes in pressure on the viscosity. Although it appears that the UA model for perfluoroalkanes is capable of predicting the relative change in viscosity with changes in state condition, the large degree to which it underpredicts the Newtonian viscosity might necessitate the use of an all-atom rather than a united-atom model, despite the increased computational cost. The inclusion of the fluorine atoms explicitly into the potential model appears to result in accurate prediction of the viscosity compared to experiment for these small perfluoroalkane molecules. However, no direct conclusions can be made as to whether all
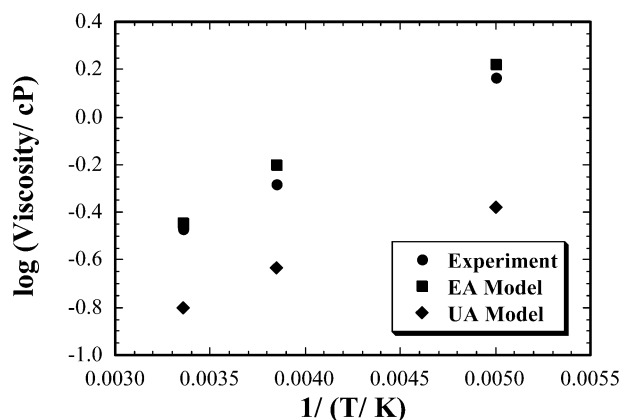
Figure 2. Influence of temperature on the viscosity of perfluorobutane.
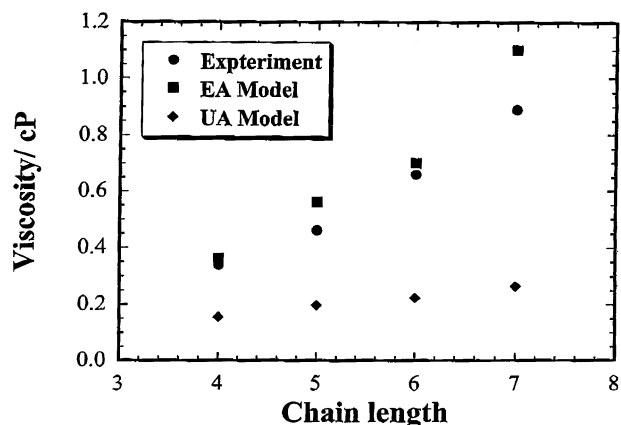
Figure 3. Influence of temperature on the viscosity of perfluorobutane.

explicit-atom models will accurately predict the viscosity of a given molecule, as the parametrization procedure undoubtedly influences the accuracy of the resulting model. However, it has been shown that the details of the torsional potential (or conformational energetics) do not influence the prediction of transport properties for such small-chain molecules.[50,64] Hence, conformational energetics should not be the reason for the EA model's accurate prediction of the viscosity.

As mentioned earlier, the UA model simulations were performed at the experimental density at atmospheric pressure for each state condition. However, because the potential model is only an approximation to the true molecular interactions, the pressure in the simulated system was not at atmospheric (the calculated pressures range from 1 to 100 atm, which seems reasonable given that pressure is very sensitive to details of the force field and the density). To determine the influence of this pressure difference on the viscosity and to compare more directly with the results of the EA model (whose simulations were carried out at the density giving a pressure of 1 atm), additional *NVT* simulations were performed for perfluorobutane at 200 and 298 K to determine the density of the system at 1 atm (which yields values of 1.73 and 1.40 g cm^{-3}, respectively) and the viscosities determined by EMD simulations ($\eta = 0.31$ cP and $\eta = 0.12$ cP at 200 and 298 K, respectively). We can see that the density corresponding to 1 atm for the UA model is lower than both the experimental value and the value used in the EA simulations. As would be expected, this causes the viscosity to deviate even further from the experimental value.

Table 3. Self-Diffusion Coefficient Estimated from EMD Simulations for Both the UA and EA Models

molecule	temperature (K)	$D \times 10^{-5}$ (cm^2 s^{-1})		
		UA	EA	UA/EA
C_4F_{10}	200	1.78	0.43	4.1
	260	3.94	1.58	2.5
	298	6.39	2.62	2.4
C_5F_{12}	215	1.81	0.42	4.3
	298	5.14	1.85	2.8
C_6F_{14}	298	4.31	1.20	3.6
	323	5.44	1.72	3.2
C_7F_{16}	298	3.89	0.81	4.8
	318	4.64	1.09	4.3

In Table 3, we present the self diffusion coefficient for each state point and molecule studied. As would be expected, for both models, the diffusion coefficient increases with increasing temperature and decreases with increasing chain length. The diffusion coefficient calculated with the UA model is seen to always be higher than that found with the EA model, which is consistent with the UA model underpredicting the viscosity relative to the EA model.

We note that the difference between the UA and EA results for the viscosity and self-diffusion coefficient become larger as the temperature decreases or the molecular weight increases. However, the UA/EA ratios for the viscosity and inverse self-diffusion coefficient remain the same, suggesting that the underestimation of the self-diffusion coefficient by the UA potential is responsible for the prediction of a lower viscosity by the UA model compared to the EA model. The larger ratio of UA/EA at low temperature is consistent with packing effects being more pronounced at low temperature, and as a result, changes in the energy landscape due to the omission of fluorine atoms has a more dramatic effect than at high temperatures.

Overall, we conclude that, to obtain accurate transport properties for perfluoroalkanes, in contrast to hydrocarbons, the greater computational expense associated with an EA model is generally justified because of the much greater reliability of the results.

Acknowledgment

Literature Cited

(1) Dobbs, A. P.; Kimberley, M. R. *J. Fluorine Chem.* **2002**, *118*, 3−17.

(2) Pabon, M.; Corpart, J. M. *J. Fluorine Chem.* **2002**, *114*, 149−156.

(3) DeSimone, J. M.; Maury, E.; Menceloglu, Y. Z.; McClain, J. B.; Romack, T. J.; Combes, J. R. *Science* **1994**, *265*, 356−359.

(4) Beckman, E. J. *Science* **1996**, *271*, 613−614.

(5) Johnston, K. P.; Harrison, K. L.; Clarke, M. J.; Howdle, S. M.; Heitz, M. P.; Bright, F. V.; Carlier, C.; Randolph, T. W. *Science* **1996**, *271*, 624−626.

(6) Jhon, M. S.; Choi, H. J. *J. Ind. Eng. Chem.* **2001**, *7*, 263−275.

(7) May, G. *Chem. Britain* **1997**, *33*, 34−36.

(8) Riess, J. G. *J. Fluorine Chem.* **2002**, *114*, 119−126.

(9) ACS *Technology Vision 2020: The U.S. Chemical Industry, A Joint Report by the American Chemical Society, American Institute of Chemical Engineers, Chemical Manufacturers Association, Council for Chemical Research and Synthetic Organic Chemical Manufacturers Association, published by the American Chemical Society*; American Chemical Society: Washington, DC, 1996.

(10) Cochran, H. D.; Cummings, P. T.; Dixon, D. A.; Golab, J. T.; Peterson, B. K.; Redondo, A.; Thompson, T. B.; Westmoreland, P. R. Chemical Industry of the Future: Technology Roadmap for Computational Chemistry. http://www.ccrhq.org/vision/index/roadmaps/CompChem Roadmap 92599.pdf.

(11) *Workshop on Predicting the Thermophysical Properties of Fluids by Molecular Simulation*; NIST: Gaithersburg, MD, 2001.

(12) Jorgensen, W. L.; Madura, J. D.; Swenson, C. J. *J. Am. Chem. Soc.* **1984**, *106*, 6638−6646.

(13) Siepmann, J. I.; Karaborni, S.; Smit, B. *J. Am. Chem. Soc.* **1993**, *115*, 6454−6455.

(14) Smith, G. D.; Jaffe, R. L.; Yoon, D. Y. *Macromolecules* **1994**, *27*, 3166−3173.

(15) Jorgensen, W. L.; Maxwell, D. S.; TiradoRives, J. *J. Am. Chem. Soc.* **1996**, *118*, 11225−11236.

(16) Nath, S. K.; Escobedo, F. A.; de Pablo, J. J.; Patramai, I. *Ind. Eng. Chem. Res.* **1998**, *37*, 3195−3202.

(17) Martin, M. G.; Siepmann, J. I. *J. Phys. Chem. B* **1998**, *102*, 2569−2577.

(18) Martin, M. G.; Siepmann, J. I. *J. Phys. Chem. B* **1999**, *103*, 4508−4517.

(19) Errington, J. R.; Panagiotopoulos, A. Z. *J. Phys. Chem. B* **1999**, *103*, 6314−6322.

(20) Chen, B.; Siepmann, J. I. *J. Phys. Chem. B* **1999**, *103*, 5370−5379.

(21) Ungerer, P.; Beauvais, C.; Delhommelle, J.; Boutin, A.; Rousseau, B.; Fuchs, A. H. *J. Chem. Phys.* **2000**, *112*, 5499−5510.

(22) Cui, S. T.; Cummings, P. T.; Cochran, H. D. *J. Chem. Phys.* **1996**, *104*, 255−262.

(23) Cui, S. T.; Gupta, S. A.; Cummings, P. T.; Cochran, H. D. *J. Chem. Phys.* **1996**, *105*, 1214−1220.

(24) Cui, S. T.; Cummings, P. T.; Cochran, H. D. *Mol. Phys.* **1996**, *88*, 1657−1664.

(25) Moore, J. D.; Cui, S. T.; Cummings, P. T.; Cochran, H. D. *AIChE J.* **1997**, *43*, 3260−3263.

(26) Cui, S. T.; Cummings, P. T.; Cochran, H. D. *Mol. Phys.* **1998**, *93*, 117−121.

(27) Cui, S. T.; Cummings, P. T.; Cochran, H. D.; Moore, J. D.; Gupta, S. A. *Int. J. Thermophys.* **1998**, *19*, 449−459.

(28) Lee, S. H.; Cummings, P. T. *Mol. Sim.* **1998**, *21*, 27−39.

(29) Cui, S. T.; Cummings, P. T.; Cochran, H. D. *J. Chem. Phys.* **1999**, *111*, 1273−1280.

(30) Moore, J. D.; Cui, S. T.; Cochran, H. D.; Cummings, P. T. *J. Chem. Phys.* **2000**, *113*, 8833−8840.

(31) McCabe, C.; Cui, S. T.; Cummings, P. T. *Fluid Phase Equilib.* **2001**, *183*, 363−370.

(32) McCabe, C.; Cui, S. T.; Cummings, P. T.; Gordon, P. A.; Saeger, R. B. *J. Chem. Phys.* **2001**, *114*, 1887−1891.

(33) McCabe, C.; Manke, C. W.; Cummings, P. T. *J. Chem. Phys.* **2002**, *116*, 3339−3342.

(34) McCabe, C.; Bedrov, D.; Smith, G. D.; Cummings, P. T. *Ind. Eng. Chem. Res.* **2001**, *40*, 473−475.

(35) Allen, W.; Rowley, R. L. *J. Chem. Phys.* **1997**, *106*, 10273−10281.

(36) Sprik, M.; Rothlisberger, U.; Klein, M. L. *J. Phys. Chem. B* **1997**, *101*, 2745−2749.

(37) Farmer, B. L.; Eby, R. K. *Polymer* **1981**, *22*, 1487−1495.

(38) Farmer, B. L.; Eby, R. K. *Polymer* **1985**, *26*, 1944−1952.

(39) Holt, D. B.; Farmer, B. L.; Macturk, K. S.; Eby, R. K. *Polymer* **1996**, *37*, 1847−1855.

(40) Holt, D. B.; Farmer, B. L. *Polymer* **1999**, *40*, 4673−4684.

(41) Holt, D. B.; Farmer, B. L. *Polymer* **1999**, *40*, 4667−4672.

(42) Rothlisberger, U.; Laasonen, K.; Klein, M. L.; Sprik, M. *J. Chem. Phys.* **1996**, *104*, 3692−3700.

(43) Sprik, M.; Rothlisberger, U.; Klein, M. L. *Mol. Phys.* **1999**, *97*, 355−373.

(44) Collazo, N.; Shin, S.; Rice, S. A. *J. Chem. Phys.* **1992**, *96*, 4735−4742.

(45) Shin, S.; Collazo, N.; Rice, S. A. *J. Chem. Phys.* **1992**, *96*, 1352−1366.

(46) Schmidt, M. E.; Shin, S.; Rice, S. A. *J. Chem. Phys.* **1996**, *104*, 2114−2123.

(47) Hariharan, A.; Harris, J. G. *J. Chem. Phys.* **1994**, *101*, 4156−4165.

(48) Cui, S. T.; Siepmann, J. I.; Cochran, H. D.; Cummings, P. T. *Fluid Phase Equilib.* **1998**, *146*, 51−61.

(49) Watkins, E. K.; Jorgensen, W. L. *J. Phys. Chem. A* **2001**, *105*, 4118−4125.

(50) Borodin, O.; Smith, G. D.; Bedrov, D. *J. Phys. Chem. B* **2002**, *106*, 9912−9922.

(51) Cui, S. T.; Cochran, H. D.; Cummings, P. T. *J. Phys. Chem. B* **1999**, *103*, 4485−4491.

(52) Salaniwal, S.; Cui, S. T.; Cummings, P. T.; Cochran, H. D. *Langmuir* **1999**, *15*, 5188−5192.

(53) Salaniwal, S.; Cui, S. T.; Cochran, H. D.; Cummings, P. T. *Langmuir* **2001**, *17*, 1773−1783.

(54) Khare, R.; de Pablo, J.; Yethiraj, A. *J. Chem. Phys.* **1997**, *107*, 6956−6964.

(55) Lahtela, M.; Linnolahti, N.; Pakkanen, T. A.; Rowley, R. L. *J. Chem. Phys.* **1998**, *108*, 2626−2630.

(56) Nosé, S. *J. Chem. Phys.* **1984**, *81*, 511−519.

(57) Tuckerman, M. E.; Berne, B. J.; Martyna, G. J. *J. Chem. Phys.* **1992**, *97*, 1990−2001.

(58) Martyna, G. J.; Tuckerman, M. E.; Tobias, D. J.; Klein, M. L. *Mol. Phys.* **1996**, *87*, 1117−1157.

(59) Ryckaert, J.; Ciccotti, G.; Berendsen, H. J. C. *J. Comput. Phys.* **1977**, *23*, 327−341.

(60) Evans, D. J.; Morriss, G. P. *Statistical Mechanics of Nonequilibrium Liquids*; Academic Press: New York, 1990.

(61) Daivis, P. J.; Evans, D. J. *J. Chem. Phys.* **1994**, *100*, 541−547.

(62) Mondello, M.; Grest, G. S. *J. Chem. Phys.* **1997**, *106*, 9327−9336.

(63) Harkins, D. *Evaluation of Available Perfluorobutane Data for Selected Physical Properties*; Oak Ridge Gaseous Diffusion Plant: Oak Ridge, TN, 1990.

(64) Mei, D.; O'Connell, J. P. *Langmuir* **2002**, *18*, 9067−9079.

(65) Van-Velzen, D.; Lopes, Langenkamp, H.; Cardozo, R. Liquid Viscosity and Chemical Constitution of Organic Compounds. A New Correlation and a Compilation of Literature data. Commission of the European Communities, 1972.